The Chromatin Structure Differentially Impacts High-Specificity CRISPR-Cas9 Nuclease Strategies

Chen, X.Y.; Liu, J.; Janssen, J.M.; Goncalves, M.A.F.V.

Molecular Therapy
Nucleic Acids
Letter to the Editor

The Chromatin Structure Differentially Impacts High-Specificity CRISPR-Cas9 Nuclease Strategies

Genome editing technologies based on RNA-guided nucleases (RGNs) derived from prokaryotic type II CRISPR-Cas9 adaptive immune systems, such as that from *Streptococcus pyogenes*[1,2] and, more recently, *Staphylococcus aureus*,[3,4] are becoming increasingly pervasive in both basic and applied research.[5,6] RGNs are ribonucleoprotein complexes whose sequence-specific guide RNA (gRNA) moieties address a Cas9 nuclease to a DNA target site (Figure S1A). Base pairing between the 5′-terminal nucleotides of the gRNA (spacer) and DNA sequences connected to a protospacer-adjacent motif (PAM), triggers Cas9-mediated double-stranded DNA break (DSB) formation.[5,6] RGNs based on *S. pyogenes* Cas9 (SpCas9) and on *S. aureus* Cas9 (SaCas9) typically have spacers with a length of 20 and 21–24 nucleotides, respectively. The PAM of SpCas9 is NGG, while that of SaCas9 is NNGRRT.[3,6] The repair of RGN-induced targeted DNA lesions by non-homologous end joining (NHEJ) or homologous recombination can result in either the deletion or addition of genetic information in cells from virtually any organism.[5,6]

Despite their ease of use and broad applicability, a major limitation of conventional RGNs is that of off-target DNA cleavage. Indeed, it has been demonstrated that up to five gRNA-DNA mismatches can be tolerated, especially when located most distally to the PAM.[7] Such mismatches can conceivably result in several hundreds of DSBs across the genome.[7] Therefore, substantial efforts have been made in recent years to minimize RGN off-target activities. These efforts resulted in a set of improved genome editing strategies, of which preeminent examples include: (1) RGNs harboring 5′-truncated gRNAs (tru-gRNAs),[8] (2) rationally designed high-specificity SpCas9 variants,[9,10] (3) offset RGN pairs containing nicking SpCas9 mutants,[11,12] and (4) repurposing of RGNs with longer PAMs, such as those from the *S. aureus* CRISPR/Cas9 system.[3,4] An overview of these approaches is presented in Figure S1.

Previous studies have shown a preferential interaction between SpCas9-based RGNs and genomic regions with euchromatic signatures.[13–17] Recently, by using cellular models based on the conditional recruitment of epigenetic remodeling complexes to isogenic target sequences, our laboratory, and that of others, have demonstrated that the activity of conventional programmable nucleases, including RGNs, can be significantly hindered by compact heterochromatin in living cells.[18,19] However, so far, the extent to which high-specificity CRISPR/Cas9 nuclease strategies are affected by higher-order chromatin topologies remains to be determined.

Hence, here, we sought to investigate and compare the impact that epigenetically regulated three-dimensional chromatin "conformers" have on the performance of the aforementioned high-specificity genome editing principles (Figure S1). In these experiments, we deployed complementary loss-of-function and gain-of-function cellular systems in which the euchromatic and heterochromatic statuses of isogenic target sequences are controlled by doxycycline (Dox).[18] These systems, based on clonal HEK.EGFP$^{TetO.KRAB}$ and polyclonal HER.TLR$^{TetO.KRAB}$ cell lines, permit the measurement of the frequencies of targeted DSBs made by different programmable nucleases through the quantification of EGFP^{-} and mCherry^{+} cells,[18,20] respectively, generated after NHEJ-mediated DSB repair (for details, see Figure 1A). In brief, reporter cells cultured without Dox (heterochromatic target sites; high H3K9me3/low H3Ac) or with Dox (euchromatic target sites; high H3Ac/low H3K9me3) are exposed to different programmable nuclease combinations.[18] After the action of the programmable nucleases takes place, all cultures receive Dox to allow for transgene expression and quantification of gene editing events (Figure 1A).

We started by comparing site-specific DSB formation by RGNs containing full-length gRNAs (FL-gRNAs) or Tru-gRNAs at euchromatic ("open") versus heterochromatic ("closed") target sequences. The former gRNAs have canonical, 20-mer spacers; the latter display shorter, mostly 18-mer to 17-mer spacers.[8] The reduced DNA-binding energies of Tru-gRNAs is thought to cause the preferential binding of the respective SpCas9 partner to fully complementary target DNA (Figure S1B).[8] Gene editing experiments were initiated by transfecting HEK.EGFP$^{TetO.KRAB}$ cells, cultured in the presence of Dox or on its absence, with plasmids encoding sets of SpCas9:FL-gRNA or SpCas9:Tru-gRNA complexes targeting five different positions along the *EGFP* ORF (Figure S2). After the action of the various RGN complexes had taken place, Dox was added to the different cell cultures for flow cytometric quantification of targeted gene knockout levels. We found that, independently of their lengths, the various RGNs had similar chromatin impact indexes (Figure 1B), as defined by the ratios between the frequencies of DSB formation at euchromatic versus heterochromatic target sites (Figure S3). Hence, despite their predicted lower DNA-binding energies, derived from a reduced Watson and Crick base-pairing potential, RGNs with Tru-gRNAs were hindered by heterochromatin to approximately the same extent as those harboring standard FL-gRNAs.

The recognition of the PAM by the PID domain of SpCas9 is the first event leading to targeted DNA cleavage.[21] After this initial genomic DNA interrogation, local double helix melting permits the nucleation of gRNA-DNA hybridization and subsequent R-loop expansion along a PAM-proximal to PAM-distal direction (i.e., 3′→5′). Finally, full-length heteroduplex formation between unwound DNA and gRNA sequences triggers phosphodiester bond hydrolysis on both strands through a concerted, PAM-dependent, allosteric activation of SpCas9's HNH and RuvC nuclease domains.[21] Based on this series of events, our data (Figure 1B) indicate that, once a catalytically competent RGN complex manages to engage a heterochromatic PAM sequence, the epigenetic barrier has, for the most part, been overcome, with the length of the gRNA posing no significant limitations to the subsequent

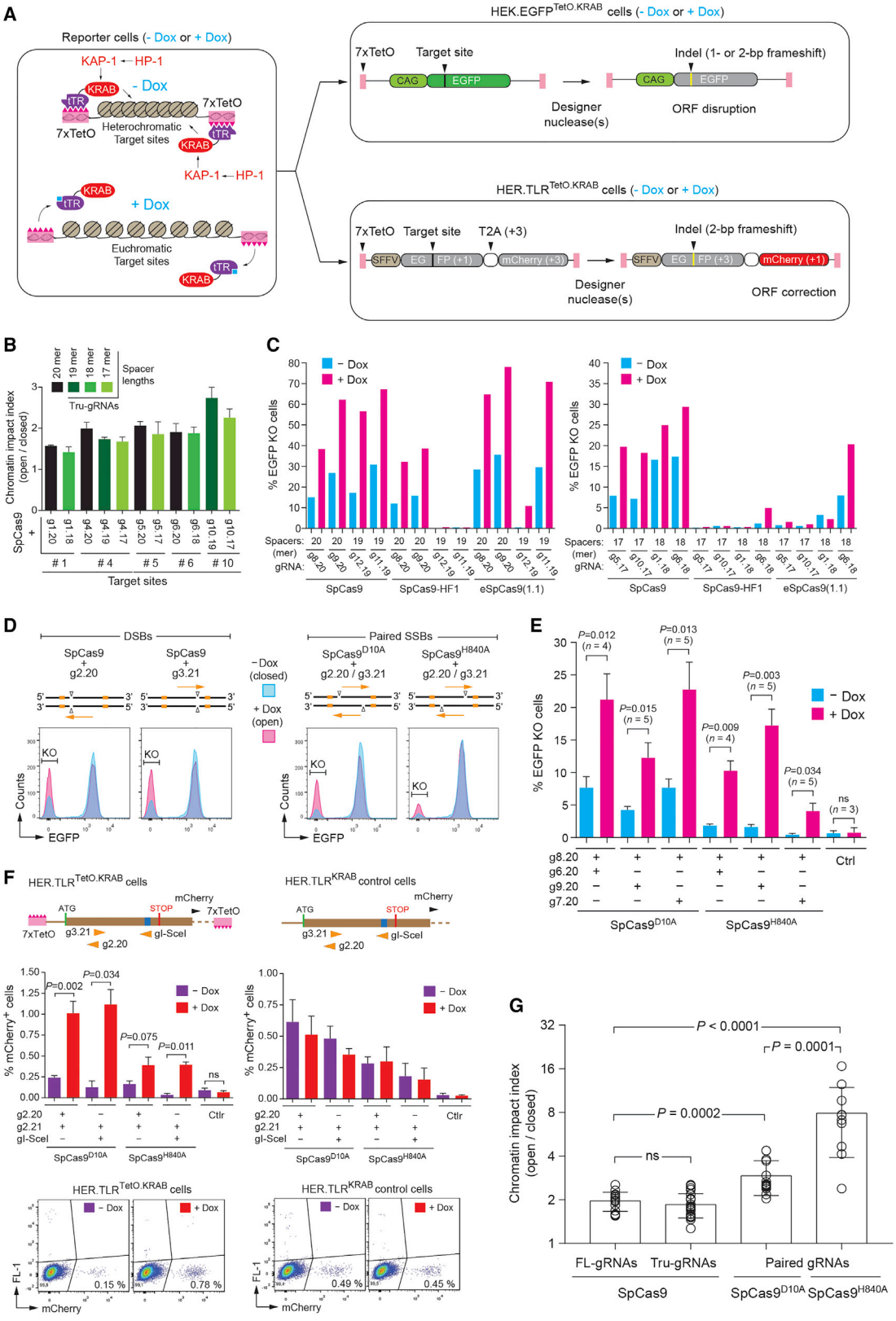

(legend on next page)

aforementioned downstream processes. As corollary, the ultimate activity of SpCas9:gRNA complexes at specific, PAM-defined, target sites seems to be primarily determined by the degree of chromatin accessibility rather than the extent of gRNA-DNA hybridization at those sites. These results bode well for using 18-mer and 17-mer Tru-gRNAs for achieving strict target DNA cleavage[8] and possibly deploying <16-mer Tru-gRNAs, which render RGNs catalytically inert, for multiplexing purposes. Indeed, the combination of these shortened, <16-mer Tru-gRNAs together with SpCas9 proteins fused to heterologous domains can be applied in a variety of orthogonal contexts, such as those involving combinatorial editing and transcriptional modulation of distinct loci in individual cells.[22,23]

In a previous study, our laboratory demonstrated that RGNs consisting of FL-gRNAs and SpCas9-HF1 or FL-gRNAs and eSpCas9(1.1) are hindered by heterochromatin[18]. Combining Tru-gRNAs with high-specificity Cas9 variant SpCas9-HF1 (Kleinstiver et al.[9]) or eSpCas9(1.1)[10] offers the prospect for further minimizing off-target DSB formation (Figure S1C). Previous experiments have, however, indicated that such Tru-gRNA-containing RGNs display reduced on-target activities when compared to those bearing FL-gRNAs.[9,10] Results presented in Figure 1C extend these findings to isogenic target sequences subjected to distinct epigenetic states. In addition, our data indicate that the compatibility between Tru-gRNAs and eSpCas9(1.1) is higher than that between Tru-gRNAs and SpCas9-HF1 in that, when compared to the former, the latter setting yielded lower gene knockout frequencies at each of the tested PAM-defined target sequences. Indeed, combining SpCas9-HF1 and Tru-gRNAs with spacers a single nucleotide shorter than 20-mer FL-gRNAs (i.e., g11.19 and g12.19) sufficed to abrogate RGN activity in cells subjected to both Dox regimens, but this was not so when applying the same Tru-gRNAs together with eSpCas9(1.1) (Figure 1C, left graph). Additional gene editing experiments using a panel of <19-mer Tru-gRNAs (i.e., g5.17, g10.17, g1.18 and g6.18) in HEK.EGFP$^{TetO.KRAB}$ cells treated and not treated with Dox confirmed the higher catalytic impairment of SpCas9-HF1:Tru-gRNA complexes over their eSpCas9(1.1):Tru-gRNA counterparts (Figure 1C, right graph).

Offset gRNA pairs addressing SpCas9 "nickases" to opposite DNA strands guarantee that DSBs are, for the most part, restricted to the bipartite target site after the local coordinated formation of SSBs (Figure S1D). Indeed, specificity gains between 200-fold to >1,500-fold have been reported for this dual RGN nicking strategy.[12] Gene editing experiments with two gRNAs (i.e., g2.20 and g3.21), whose target sequences partially overlap (Figure S2), were individually combined with wild-type SpCas9 (controls) or mixed together with SpCas9^{D10A} or with SpCas9^{H840A}. These experiments validated HEK.EGFP$^{TetO.KRAB}$ cells as a readout system for assessing the impact of chromatin on dual RGN "nickases" (Figure 1D). Albeit dependent on two different gRNAs, dual RGN "nickases" display a higher theoretical coverage of the genomic landscape when compared to that of conventional RGNs and other dimeric programmable nucleases, such as zinc-finger nucleases.[5] This stems from the fact that dual RGN "nickases" are compatible with a broad range of DNA spacing between the target sites of their individual members (i.e., about –4-bp to +100-bp), which, in turn, increases the chances for locating suitable PAMs. Hence, to exploit this feature, in subsequent gene

Figure 1. Assessing the Effect of Alternative Chromatin Topologies on High-Specificity CRISPR/Cas9 Nucleases Based on SpCas9 Proteins

(A) Cellular reporter systems for tracking programmable nuclease-induced DSB formation at isogenic target sequences possessing different chromatin conformations. Left panel: the binding of tTR-KRAB fusion proteins to *TetO* elements triggers heterochromatin spread after the recruitment of endogenous epigenetic remodeling complexes composed of, among others, KAP1 and HP1. The addition of doxycycline (Dox) alters the tTR-KRAB conformation, preventing its interaction with the *TetO* elements, resulting in the transition of the associated DNA sequences from a compact/heterochromatic into a relaxed/euchromatic state. Top right panel: schematics of the HEK.EGFP$^{TetO.KRAB}$ loss-of-function system. The tTR-KRAB-expressing human embryonic kidney cells HEK.EGFP$^{TetO.KRAB}$ harbor a *TetO*-flanked *EGFP* expression unit. In this construct, an in-frame *EGFP* reporter can be placed out of frame after indel formation by NHEJ-mediated repair of site-specific DSBs. Thus, non-fluorescent cells report sequence-specific nuclease activity. Bottom right panel: diagram of the HER.TLR$^{TetO.KRAB}$ gain-of-function system. The tTR-KRAB-expressing human embryonic retinoblasts HER.TLR$^{TetO.KRAB}$ contain a Traffic Light Reporter (*TLR*)[20] flanked by *TetO* elements (*TLR*^{TetO}).[18] In this construct, an out-of-frame *mCherry* ORF linked to a *T2A* sequence and an *EGFP* ORF with a disrupting I-SceI recognition site, can be placed in-frame after indel formation by NHEJ-mediated repair of targeted DSBs. Hence, in this case, the resulting red fluorescent cells are those reporting sequence-specific nuclease activity. (B) Chromatin impact indexes of RGNs with full-length and truncated gRNAs. HEK.EGFP$^{TetO.KRAB}$ cells, treated and not treated with Dox, were exposed to SpCas9 together with the indicated gRNAs. The chromatin impact index for each RGN was determined by dividing the *EGFP* knockout levels measured at euchromatic by those gauged at heterochromatic conditions (i.e., +Dox and –Dox, respectively). Error bars indicated mean ± SD (n = 3 independent experiments done on different days). (C) Testing the impact of chromatin on RGNs consisting of high-specificity Cas9 variants and Tru-gRNAs. HEK.EGFP$^{TetO.KRAB}$ cells, incubated in the presence and in the absence of Dox, received the indicated nuclease-gRNA pairs. Targeted mutagenesis levels at euchromatic (+Dox) and heterochromatic (−Dox) target sequences were quantified by EGFP-directed flow cytometry. The bars in both graphs correspond to an individual experiment using RGNs with FL-gRNAs (n = 2) or Tru-gRNAs (n = 6) (D) Validation of HEK.EGFP$^{TetO.KRAB}$ cells for assessing paired RGN "nickases". HEK.EGFP$^{TetO.KRAB}$ cells, treated and not treated with Dox, were exposed to SpCas9 and single gRNAs (DSBs) or SpCas9 nicking mutants together with two partially overlapping gRNAs (paired SSBs). Cell fractions with *EGFP* knockout (KO) alleles are indicated in the flow cytometry histograms. (E) Screening dual RGN "nickase" activities at euchromatic versus heterochromatic target sequences. HEK.EGFP$^{TetO.KRAB}$ cells, treated and not treated with Dox, were exposed to the specified dual RGN "nickases". The frequencies of targeted mutagenesis under both Dox regimens were determined by EGFP-directed flow cytometry. Error bars indicate mean ± SEM, corresponding to independent experiments (n) performed on different days. (F) Testing of dual RGN nicking complexes on the gain-of-function reporter system. HER.TLR$^{TetO.KRAB}$ and control HER.TLR^{KRAB} cells, incubated in the presence and absence of Dox, received the indicated dual RGN "nickases". The frequencies of DSB-induced ORF correction under both Dox regimens were determined by mCherry-directed flow cytometry. Error bars indicate mean ± SEM. A minimum of two and a maximum of four independent experiments were carried out. Representative flow cytometry dot plots of these experiments are presented below each graph. (G) Comparison of chromatin impact indexes between conventional and high-specificity RGN complexes. Scatterplot with bar, gathers the datasets obtained from gene editing experiments carried out in HEK.EGFP$^{TetO.KRAB}$ cells.

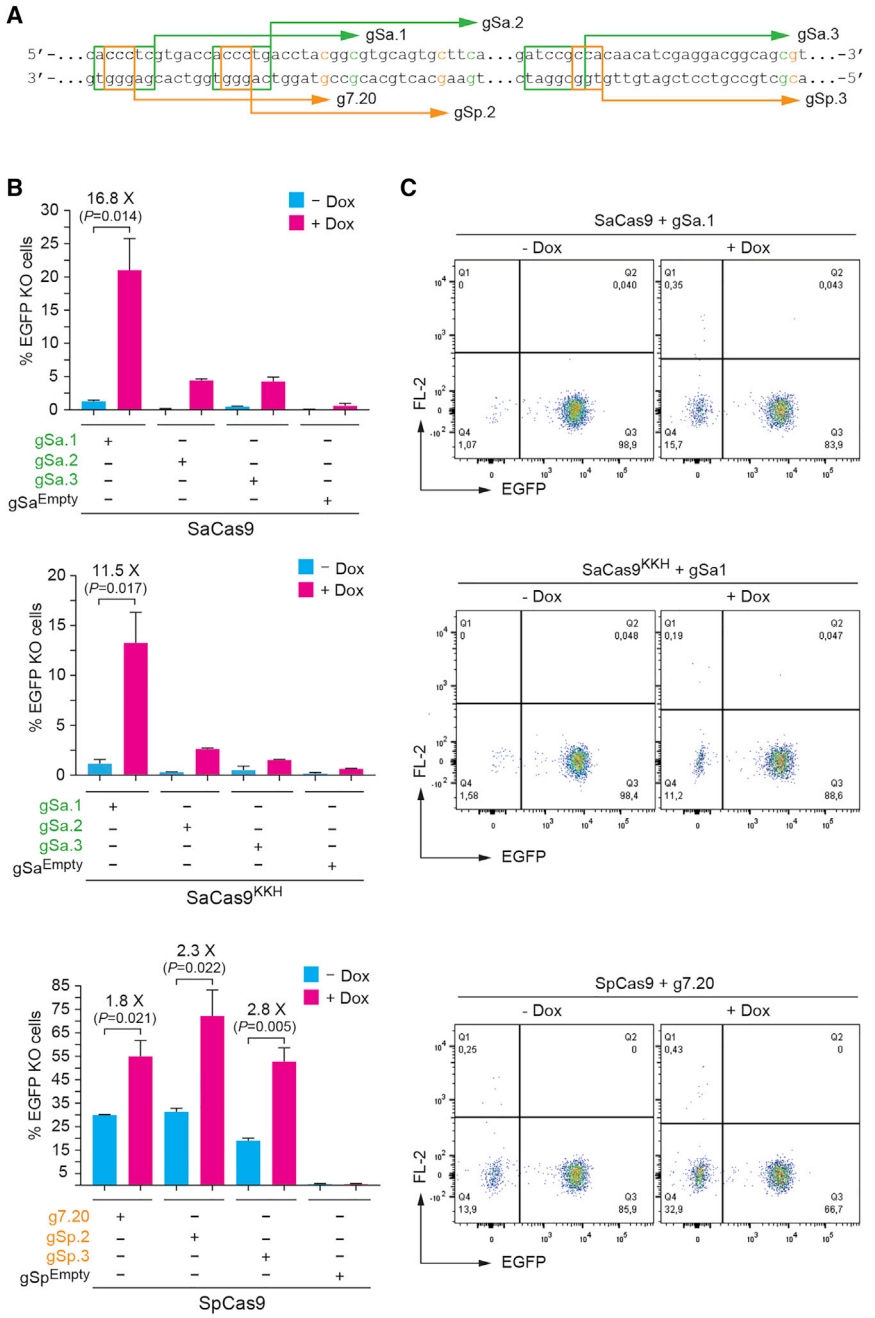

Figure 2. Assessing the Effect of Alternative Chromatin Conformations on CRISPR/Cas9 Nucleases Based on SaCas9 Proteins

(A) Target sequences of RGNs consisting of SaCas9:gRNA or SpCas9:gRNA complexes. The sequences complementary to the *S. aureus* and *S. pyogenes* gRNAs are indicated underneath the green and orange arrows, respectively. The sequences corresponding to the PAMs of *S. aureus* and *S. pyogenes* RGNs are highlighted by green and orange boxes, respectively. (B) Testing the effect of chromatin on RGNs harboring SaCas9, SaCas9^{KKH}, or SpCas9. HEK.EGFP$^{TetO.KRAB}$ cells, incubated in the presence and absence of Dox, received the indicated nuclease-gRNA pairs. Targeted mutagenesis levels at euchromatic (+Dox) and heterochromatic (−Dox) target sequences were quantified by EGFP-directed flow cytometry. Error bars correspond to mean ± SD (n = 3 independent experiments performed on different days). (C) Representative flow cytometry dot plots of HEK.EGFP$^{TetO.KRAB}$ cells treated with the indicated experimental conditions.

editing experiments performed in HEK. EGFP$^{TetO.KRAB}$ cells, we focused on using sets of gRNA pairs (i.e. g8.20/g6.20, g8.20/g9.20, and g8.20/g7.20) with non-overlapping target sequences (Figure S2). Flow cytometric quantification of EGFP^{-} cells generated in HEK.EGFP$^{TetO.KRAB}$ cultures after NHEJ-mediated DSB repair revealed that dual RGN "nickases" were significantly impaired at heterochromatic target sites (Figure 1E). This was independent of the nicking SpCas9 mutant used and, therefore, independent of the type of single-stranded DNA overhangs generated (Figure 1E). Similar results were obtained after flow cytometric quantification of mCherry^{+} cells in HER.TLR$^{TetO.KRAB}$ cultures subjected to both Dox regimens and exposed to different gRNA pairs (i.e., g2.20/gI-SceI and g2.21/gI-SceI) combined with each of the two nicking SpCas9 mutants (Figure 1F and Figure S4). Importantly, there were no significant Dox-dependent differences in the frequencies of mCherry^{+} cells in control, *TetO*$^{-}$, HER.TLR^{KRAB} cultures subjected to the same experimental conditions that had been applied to HER.TLR$^{TetO.KRAB}$ cultures. Taken together, these experiments show that, in contrast to RGNs containing TrugRNAs, dual RGN "nickases" are significantly more affected by heterochromatin than conventional RGNs (Figure 1G). We speculate that, when heterochromatinized, the intervening sequences separating the two opposite SSBs made by dual RGN "nickases" might become more resistant to double helix denaturation when compared to their euchromatinized isogenic counterparts. Interestingly, of the two types of dual RGN "nickases," those based on SpCas9^{D10A} are the least hindered by heterochromatin. SpCas9^{D10A} cuts the DNA strand complementary to the gRNA, whereas SpCas9^{H840A} cleaves the non-complementary strand. Moreover, in contrast to SpCas9^{D10A}, SpCas9^{H840A} has 3′ to 5′ exonuclease activity.[2] Whether these or other biochemical traits underlie the observed differential impact of heterochromatin on the activity of these dual RGN "nickases" will be worthy of further investigation.

The relatively small size of the SaCas9 coding sequence (3.3 Kb) permits its

incorporation, together with regulatory elements and gRNA expression units, into viral vector particles with limited packaging capacity, such as those of commonly used adeno-associated viral vectors.[3] In addition, SaCas9-based RGNs increase gene editing versatility by permitting orthogonal (epi) genetic manipulations and potentially offer a higher degree of target site specificity owing to their extended spacer and PAM sequences. Recently, a molecular evolution strategy led to the selection of a SaCas9 variant with an expanded targeting range, i.e., SaCas9^{KKH} (PAM = NNNRRT instead of NNGRRT), further increasing the versatility of SaCas9-based RGNs.[4] As of yet, the impact of chromatin on these new gene editing tools has not been studied. Therefore, we next carried out gene editing experiments in HEK.EGFP$^{TetO.KRAB}$ cells using SaCas9:gRNA and SaCas9^{KKH}:gRNA complexes targeting three different *EGFP* sites embedded in euchromatin or heterochromatin (Figure 2A). As references, we also targeted each of these target sequences with prototypic SpCas9:gRNA complexes (Figure 2A). Results presented in Figures 2B and 2C reveal that the SaCas9 RGNs were clearly hindered by heterochromatin. In fact, in contrast to SpCas9 RGNs, at heterochromatin, SaCas9 RGNs yielded frequencies of *EGFP* knockout that were at or only slightly above background levels.

We conclude that the higher-order chromatin environment is an important parameter to take into consideration while selecting and designing the tools and strategies underlying precise genome editing based on high-specificity CRISPR/Cas9 nuclease complexes.

SUPPLEMENTAL INFORMATION

Supplemental Information includes Supplemental Materials and Methods, nine figures, and nine tables and can be found with this article online at http://dx.doi.org/10.1016/j.omtn.2017.08.005.

AUTHOR CONTRIBUTIONS

X.C. generated and characterized reagents, performed experiments, analyzed the data, and wrote the paper together with M.A.F.V.G.; J.L. generated reagents, performed experiments, and analyzed the data; J.M.J. generated reagents and analyzed the data. M.A.F.V.G. designed the study, analyzed the data, and wrote the paper together with X.C.

CONFLICTS OF INTEREST

The authors declare no conflict of interest.

ACKNOWLEDGMENTS

The authors thank Rob Hoeben and Ignazio Maggio (Leiden University Medical Center, Departments of Molecular Cell Biology and Pediatrics, respectively) for their critical reading of the manuscript. This work was partially supported by the Dutch Prinses Beatrix Spierfonds (W.OR11–18) and ProQR Therapeutics (Leiden, the Netherlands). X.C. holds a Ph.D. research grant from the China Scholarship Council-Leiden University Joint Scholarship Programme.

Xiaoyu Chen,[1] Jin Liu,[1] Josephine M. Janssen,[1] and Manuel A.F.V. Gonçalves[1]

[1]Department of Molecular Cell Biology, Leiden University Medical Centre, Einthovenweg 20, 2333 ZC Leiden, the Netherlands

http://dx.doi.org/10.1016/j.omtn.2017.08.005

Correspondence: Manuel A.F.V. Gonçalves, Department of Molecular Cell Biology, Leiden University Medical Centre, Einthovenweg 20, 2333 ZC Leiden, the Netherlands.
E-mail: m.f.v.goncalves@lumc.nl

REFERENCES

1. Gasiunas, G., Barrangou, R., Horvath, P., and Siksnys, V. (2012). Cas9-crRNA ribonucleoprotein complex mediates specific DNA cleavage for adaptive immunity in bacteria. Proc. Natl. Acad. Sci. USA *109*, E2579–E2586.
2. Jinek, M., Chylinski, K., Fonfara, I., Hauer, M., Doudna, J.A., and Charpentier, E. (2012). A programmable dual-RNA-guided DNA endonuclease in adaptive bacterial immunity. Science *337*, 816–821.
3. Ran, F.A., Cong, L., Yan, W.X., Scott, D.A., Gootenberg, J.S., Kriz, A.J., Zetsche, B., Shalem, O., Wu, X., Makarova, K.S., et al. (2015). In vivo genome editing using Staphylococcus aureus Cas9. Nature *520*, 186–191.
4. Kleinstiver, B.P., Prew, M.S., Tsai, S.Q., Nguyen, N.T., Topkar, V.V., Zheng, Z., and Joung, J.K. (2015). Broadening the targeting range of Staphylococcus aureus CRISPR-Cas9 by modifying PAM recognition. Nat. Biotechnol. *33*, 1293–1298.
5. Maggio, I., and Gonçalves, M.A. (2015). Genome editing at the crossroads of delivery, specificity, and fidelity. Trends Biotechnol. *33*, 280–291.
6. Wright, A.V., Nuñez, J.K., and Doudna, J.A. (2016). Biology and Applications of CRISPR Systems: Harnessing Nature's Toolbox for Genome Engineering. Cell *164*, 29–44.
7. Carroll, D. (2013). Staying on target with CRISPR-Cas. Nat. Biotechnol. *31*, 807–809.
8. Fu, Y., Sander, J.D., Reyon, D., Cascio, V.M., and Joung, J.K. (2014). Improving CRISPR-Cas nuclease specificity using truncated guide RNAs. Nat. Biotechnol. *32*, 279–284.
9. Kleinstiver, B.P., Pattanayak, V., Prew, M.S., Tsai, S.Q., Nguyen, N.T., Zheng, Z., and Joung, J.K. (2016). High-fidelity CRISPR-Cas9 nucleases with no detectable genome-wide off-target effects. Nature *529*, 490–495.
10. Slaymaker, I.M., Gao, L., Zetsche, B., Scott, D.A., Yan, W.X., and Zhang, F. (2016). Rationally engineered Cas9 nucleases with improved specificity. Science *351*, 84–88.
11. Mali, P., Aach, J., Stranges, P.B., Esvelt, K.M., Moosburner, M., Kosuri, S., Yang, L., and Church, G.M. (2013). CAS9 transcriptional activators for target specificity screening and paired nickases for cooperative genome engineering. Nat. Biotechnol. *31*, 833–838.
12. Ran, F.A., Hsu, P.D., Lin, C.Y., Gootenberg, J.S., Konermann, S., Trevino, A.E., Scott, D.A., Inoue, A., Matoba, S., Zhang, Y., and Zhang, F. (2013). Double nicking by RNA-guided CRISPR Cas9 for enhanced genome editing specificity. Cell *154*, 1380–1389.
13. Kuscu, C., Arslan, S., Singh, R., Thorpe, J., and Adli, M. (2014). Genome-wide analysis reveals characteristics of off-target sites bound by the Cas9 endonuclease. Nat. Biotechnol. *32*, 677–683.
14. Wu, X., Scott, D.A., Kriz, A.J., Chiu, A.C., Hsu, P.D., Dadon, D.B., Cheng, A.W., Trevino, A.E., Konermann, S., Chen, S., et al. (2014). Genome-wide binding of the CRISPR endonuclease Cas9 in mammalian cells. Nat. Biotechnol. *32*, 670–676.
15. Polstein, L.R., Perez-Pinera, P., Kocak, D.D., Vockley, C.M., Bledsoe, P., Song, L., Safi, A., Crawford, G.E., Reddy, T.E., and Gersbach, C.A. (2015). Genome-wide specificity of DNA binding, gene regulation, and chromatin remodeling by TALE- and CRISPR/Cas9-based transcriptional activators. Genome Res. *25*, 1158–1169.
16. O'Geen, H., Henry, I.M., Bhakta, M.S., Meckler, J.F., and Segal, D.J. (2015). A genome-wide analysis of Cas9 binding specificity using ChIP-seq and targeted sequence capture. Nucleic Acids Res. *43*, 3389–3404.
17. Horlbeck, M.A., Witkowsky, L.B., Guglielmi, B., Replogle, J.M., Gilbert, L.A., Villalta, J.E., Torigoe, S.E., Tjian, R., and Weissman, J.S. (2016). Nucleosomes impede Cas9 access to DNA in vivo and in vitro. eLife *5*, e12677.
18. Chen, X., Rinsma, M., Janssen, J.M., Liu, J., Maggio, I., and Gonçalves, M.A. (2016). Probing the impact of chromatin conformation on genome editing tools. Nucleic Acids Res. *44*, 6482–6492.
19. Daer, R.M., Cutts, J.P., Brafman, D.A., and Haynes, K.A. (2017). The impact of chromatin dynamics on

Cas9-mediated genome editing in human cells. ACS Synth. Biol. *6*, 428–438.

20. Certo, M.T., Ryu, B.Y., Annis, J.E., Garibov, M., Jarjour, J., Rawlings, D.J., and Scharenberg, A.M. (2011). Tracking genome engineering outcome at individual DNA breakpoints. Nat. Methods *8*, 671–676.

21. Sternberg, S.H., Redding, S., Jinek, M., Greene, E.C., and Doudna, J.A. (2014). DNA interrogation by the CRISPR RNA-guided endonuclease Cas9. Nature *507*, 62–67.

22. Dahlman, J.E., Abudayyeh, O.O., Joung, J., Gootenberg, J.S., Zhang, F., and Konermann, S. (2015). Orthogonal gene knockout and activation with a catalytically active Cas9 nuclease. Nat. Biotechnol. *33*, 1159–1161.

23. Kiani, S., Chavez, A., Tuttle, M., Hall, R.N., Chari, R., Ter-Ovanesyan, D., Qian, J., Pruitt, B.W., Beal, J., Vora, S., et al. (2015). Cas9 gRNA engineering for genome editing, activation and repression. Nat. Methods *12*, 1051–1054.